Systematic investigation of the phase behavior in binary fluid mixtures. I. Calculations based on the Redlich–Kwong equation of state

Ulrich K. Deiters
Lehrstuhl für Physikalische Chemie II, Ruhr-Universität Bochum, D-4630 Bochum 1, Federal Republic of Germany

Ian L. Pegg
Physics Department, The Catholic University of America, Washington, D. C. 20064

(Received 29 September 1988; accepted 16 February 1989)

The original Redlich–Kwong equation, together with the usual quadratic mixing rules, has been used to calculate phase diagrams for binary fluid mixtures and to classify them according to the system of van Konynenburg and Scott. Global phase diagrams (maps) showing the extent of the various phase diagram classes in the space of the Redlich–Kwong parameters are presented. While for molecules of equal size the results are very similar to those known for the van der Waals equation, the maps become topologically different for molecules of unequal sizes; some complicated phase diagram classes, which otherwise cover small domains on the maps or cannot be found at all, become quite important.

INTRODUCTION

The calculation of fluid phase equilibria in mixtures by means of equations of state is a well established and frequently used method, especially when fluids under elevated pressures are concerned. Almost two decades ago, Scott and van Konynenburg[1,2] showed that almost all known kinds of fluid phase equilibria—vapor–liquid, liquid–liquid, and gas–gas—can be generated, at least qualitatively, from the van der Waals equation of state combined with the van der Waals mixing rules. Only one phase equilibrium type, the so-called class VI, which occurs in some strongly polar systems, required special mixing rules. Furman *et al.*[3] made a similar study of a lattice–gas mixture and in extending that work to van der Waals mixtures Furman and Griffiths[4] identified several new classes of phase behavior. Many of these complex classes occur in regions of parameter space in which special symmetries exist. These findings essentially completed the knowledge of van der Waals mixtures of equal-sized components and the results were summarized by van Konynenburg and Scott[5] in an extensive review.

In view of the hundreds of different equations of state and mixing rules which are in use nowadays, it is rather surprising that similar investigations for more realistic, modern equations seem to be more the exception than the rule. Three publications that have to be mentioned in this context are:

—a publication by Clancy, Gubbins, and Gray.[6] This work focuses on the influence of polar forces on phase behavior; it does not include an investigation of all possible phase diagrams with their computation method.

—a publication by Jackson, Rowlinson, and Lang[7] involving a van der Waals-type equation with an improved repulsion term (hard sphere mixture). It is mostly concerned with mixtures of components with rather extreme size ratios. It covers an important, but small part of the total interaction parameter domain.

—a series of publications by Mazur and Boshkov[8–10] dealing with the global phase behavior of Lennard-Jones fluids. This work involves a systematic and thorough topological analysis of global phase diagrams. Most of the published calculations, however, are concerned with properties of mixtures with equal-sized molecules.

The knowledge about global phase diagrams and their relationship to equations of state and mixing rules is, therefore, rather sparse. It is the aim of this work to investigate the global phase behavior of a practically useful equation of state, giving special attention to mixtures of molecules of dissimilar size.

For this work, the Redlich–Kwong equation[11] has been chosen as the principal equation of state. There a three reasons for this choice:

—The Redlich–Kwong equation has often been used for engineering applications, and its phase behavior is certainly of some practical interest.

—This equation of state is simple and does not create too many numerical problems.

—Finally, the Redlich–Kwong equation is able to generate critical states of binary fluid mixtures in good quantitative agreement with experimental data.[12]

CLASSIFICATION OF PHASE DIAGRAMS

Description of classes

In order to facilitate the comparison between the behavior of Redlich–Kwong mixtures and that of van der Waals mixtures as reported by van Konynenburg and Scott, we adopt their classification system. For the reader's convenience, this system is described here in a very compressed form.

Phase diagrams of fluid mixtures are classified primarily with respect to the number and topology of the critical lines. Naturally, critical lines may originate at the critical points of the pure components; these will be named C_l and C_h, with "l" and "h" referring to the substance with the lower or higher critical temperature, respectively. It is often convenient to imagine a third critical point C_m at extremely high pressures. In the terminology of a three-component lattice gas model, where the third species represents "holes," C_l is a critical point involving component l and holes in the

 0021-9606/89/116632-10$02.10

absence of species h, whereas C_m is a critical point in a dense mixture of l and h in the absence of holes. Then, according to the system of Scott and van Konynenburg, there are six main classes (compare Fig. 1):

I an uninterrupted critical line between C_l and C_h;

II one critical line connecting C_l and C_h, another line going from C_m to a critical endpoint;

III one critical line going from C_l to an upper critical endpoint, another line going from C_h to C_m;

IV one critical line going from C_l to an upper critical endpoint, a second critical line going from C_h to a lower critical endpoint, a third line going from C_m to an upper critical endpoint.

Here two important subclasses can be distinguished from the topology of the three-phase (llg or "liquid–liquid–gas") lines (see Fig. 14, later):

IV (standard type) is a class where an llg curve connects the endpoints of the critical lines coming from C_l and from C_h.

IV* is a class where an llg curve connects the endpoints of the critical lines coming from C_h and from C_m;

V one critical line from C_l to an upper critical endpoint, another critical line from C_h to a lower critical endpoint;

VI one critical line for the vapor–liquid equilibria, another line going from a lower critical endpoint to an upper critical endpoint, and sometimes a third critical line at high pressures above the second one; the existence of additional critical line (C_m to an upper critical endpoint) has been discussed.[10]

It is rather surprising that class VI-like behavior is found in recent work on Lennard-Jones mixtures[8–10] in view of the observation that such behavior is otherwise invariably associated with mixtures in which strong hydrogen bonding or other unusually strong or specific orientational forces are present.[13] This conclusion is supported by calculations on lattice[14,15] and other models.[16] It may be worth pointing out in this context that the Lennard-Jones calculations are based on a polynomial equation of state derived from a fit to computer simulation data.

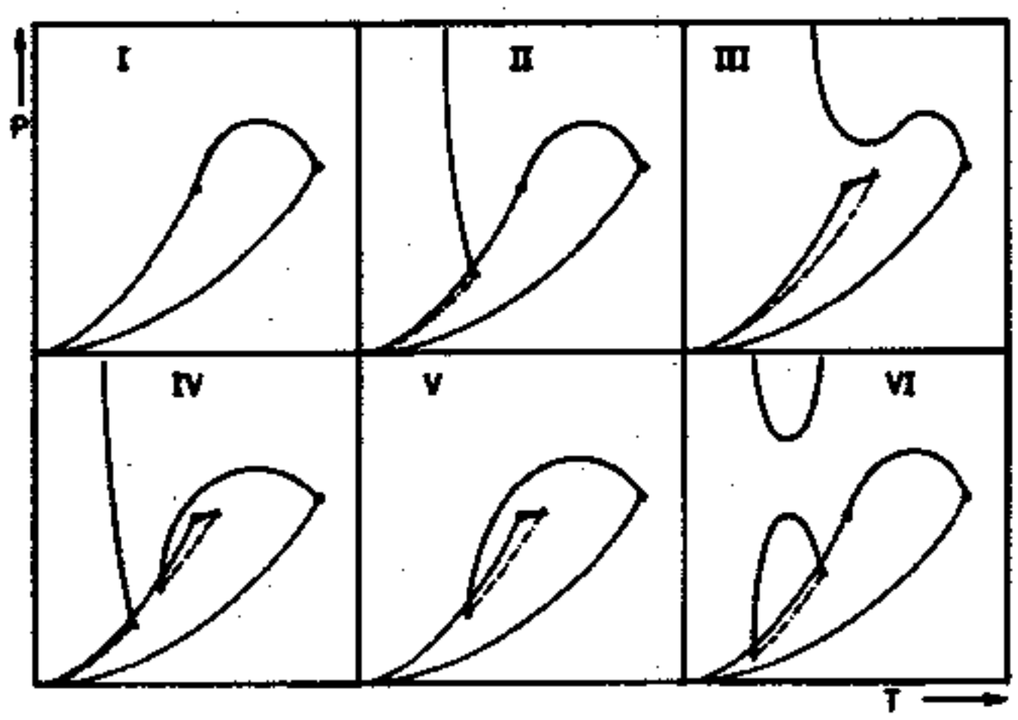

FIG. 1. Schematic representation of the main phase diagram classes. ○: pure substance critical point, △: upper critical endpoint, ▽: lower critical endpoint, ●: tricritical point, *: double critical endpoint, —: vapor pressure line, ——: critical line, -·-: three-phase line, □: four-phase state.

Recently an additional phase diagram type, VII, has been found for Lennard-Jones mixtures of equal-sized molecules.[10] It is similar to class VI, except that the critical lines originating at C_l and C_h do not meet, but are connected by a three-phase line (as in class V). However, whether the vapor-liquid critical line connects C_l and C_h or not, is a point of little practical importance; most real systems exhibiting class VI behavior would decompose because of the high temperatures associated with this critical line.

These classes can be divided into subclasses by considering additional characteristics of phase diagrams, e.g., the existence of azeotropy or heteroazeotropy (indicated by adding "-A" or "-H" to the class number). A further subdivision can be made on the occurrence of temperature or pressure minima along critical lines. This can be quite important for the construction of isothermal or isobaric equilibrium diagrams, but this subdivision is not the immediate object of this work.

Under special circumstances the standard classes II and III are transformed into the classes II-A*, III*, III-A*, and III-A**. The phase diagrams of these classes contain an additional critical line running from an upper critical endpoint to another upper critical endpoint; furthermore, the three-phase lines meet at a four-phase point. Class II-A* is always associated with azeotropy; there does not seem to be a plain class II*. The special subclasses of III differ from each other with respect to azeotropy: For III-A* the critical azeotrope is on the new critical line, for III-A** it is on the critical line originating from C_l (Fig. 2), and for plain III* there is no azeotropy.

It is important to realize that this classification is based on fluid phase equilibria only; solid–fluid equilibria are not accounted for.

Boundaries between classes

We have found no evidence for the existence of class VI (or VII) in Redlich–Kwong mixtures, as would be expected on the basis of the foregoing discussion. These classes are therefore left out of the following considerations.

A thermodynamic analysis of the phase diagram classes shows that the classification into five main classes is not due to a single (pentavalent) criterion, but that there are at least three different criteria.

Tricritical states

The strongest criterion is responsible for the distinction between the classes I and V, or II and IV, or III and IV*. The

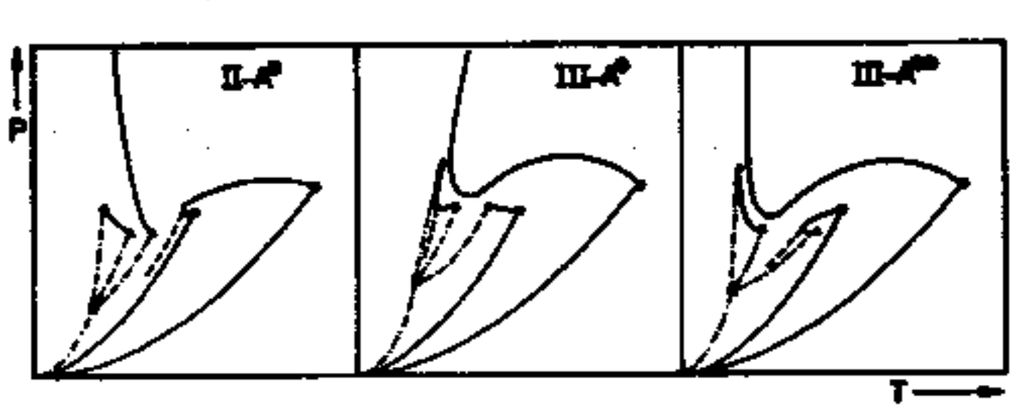

FIG. 2. Schematic representation of the phase diagram classes in the shield region. For an explanation of symbols see Fig. 1.

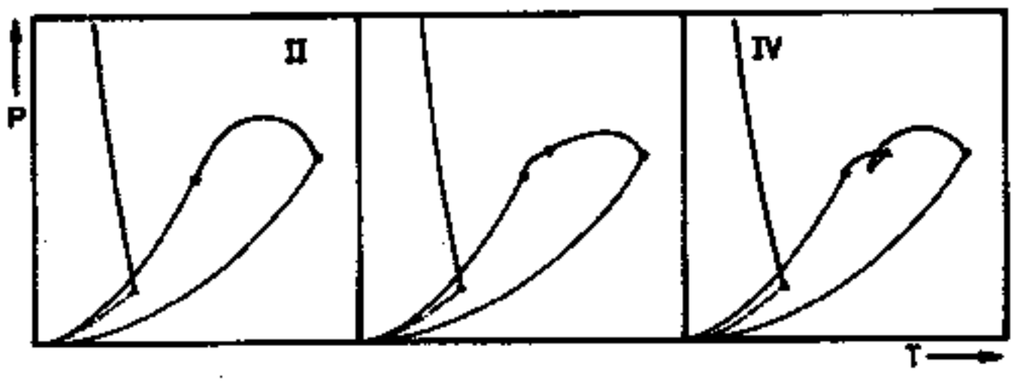

FIG. 3. Tricritical point as transition state between class II and IV. For an explanation of symbols see Fig. 1.

difference between these classes lies in the fact that in one case the critical points C_l and C_h are connected by a critical line, but in the other case not. The "transition state" would be represented by a phase diagram where the three-phase line connecting the two critical lines in class V, IV, or IV* shrinks to zero length at a tricritical point (Fig. 3). The mathematical criterion for a tricritical point is

$$G_{2x} = G_{3x} = G_{4x} = G_{5x} = 0 . \tag{1}$$

G_{kx} is a shorthand notation for $(\partial^k G_m/\partial x_1^k)_{P,T}$.

Double critical endpoints

When the critical lines of a class IV mixture are calculated it often turns out that there are only two separate critical lines, rather than three. The critical line originating at C_h passes through a very pronounced pressure minimum before going to high pressures. If the minimum lies below the three-phase line, or even at negative pressure, the critical line becomes unstable and appears to be interrupted, thereby producing class IV behavior. This means that class IV is often a distorted class III. The transition state between class IV and class III (or II and IV*) is a phase diagram where the critical line just touches the three-phase line forming a double critical endpoint (Fig. 4). At a double critical endpoint there is a critical phase in equilibrium with another (noncritical) phase, and the slopes of the critical line and the three-phase line are the same. This leads to the following equations for a double critical endpoint (critical phase denoted by "c," auxiliary equilibrium phase by "a"):

$$G_{2x}^c = G_{3x}^c = 0 \quad \text{(criticality)}, \tag{2}$$

$$\mu_i^c = \mu_i^a \quad i = 1,2 \quad \text{(phase equilibrium)}, \tag{3}$$

$$\frac{S_{2x}^c}{V_{2x}^c} = \frac{S_m^c - S_m^a - (x_1^c - x_1^a)S_x^c}{V_m^c - V_m^a - (x_1^c - x_1^a)V_x^c} \quad \text{(slope criterion)}. \tag{4}$$

The notation for the derivatives S_x, S_{2x}, V_x, and V_{2x} is analogous to that for G_{2x}. These derivatives must be calculated at constant pressure and temperature. A method of computation is given in the Appendix.

Zero-temperature endpoints

The classes I and II, or IV and V, differ in the existence of a liquid–liquid critical line, which goes from high pressures to an upper critical endpoint. It is difficult to give a mathematical criterion for the existence of such a critical line. For the transition state between class I and class II one might suggest a phase diagram where the low-temperature critical endpoint has a temperature of zero. Since at this temperature the pressure of the three-phase state llg would also be zero, the molar volume would converge to the covolume. Under these cirumstances only the attractive term of the equation of state contributes to the curvature of G_m vs x_1. The zero-temperature endpoint is then defined by

$$G_{2x} = G_{3x} = 0 \quad \text{at } P,T \to 0 . \tag{5}$$

Computational details are given in the Appendix. This criterion is not completely satisfactory since it is highly hypothetical. Crystallization will put an end to fluid phase equilibria long before the zero-temperature endpoint is reached. Therefore criterion (5) cannot be used to predict the practical existence of a liquid–liquid critical line; it can, of course, be used to exclude it.

Stability

The equations given above represent only the necessary conditions for the calculation of boundaries between regions in the global phase diagram. Not all solutions to these equations are acceptable tricritical states, double critical endpoints, etc.; The following stability criteria must also be imposed in order to identify the physically meaningful solutions:

—thermal stability: $T > 0$. (6)

This is inherent in the Redlich–Kwong equation.

—Mechanical stability: $P > 0$;(7) (7)

$$A_{2\nu} > 0. \tag{8}$$

$A_{2\nu}$ may vanish only at the critical points of the pure substances and in the case of critical azeotropy.

—local diffusion stability: $G_{4x} > 0$, (9a)

(for tricritical states: $G_{6x} > 0$). (9b)

Fluids disobeying this relation are unstable against concentration fluctuations.

—Global diffusion stability:

$$x_1^a(\mu_1^a - \mu_1^c) + x_2^a(\mu_2^a - \mu_2^c) > 0. \tag{10}$$

This criterion compares the molar Gibbs energy of an auxiliary phase with the extrapolated value from a tangent to the critical state. The above relation must hold for all mole fractions $x_1^a \cdot \mu_i^c$ is evaluated at the critical mole fraction x_1^c, and μ_i^a at x_1^a. Fluids disobeying this relation are metastable against phase separation.

Mechanically unstable states were always immediately discarded by our computer programs. Many of the following

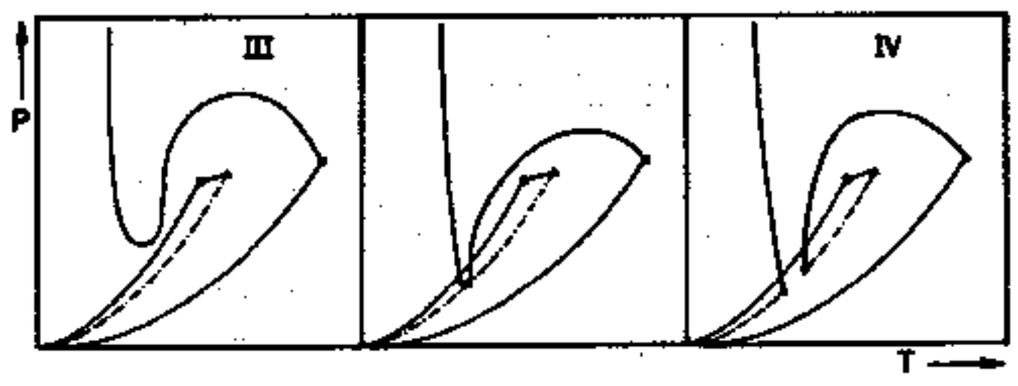

FIG. 4. Critical double endpoint as transition state between class and IV. For an explanation of symbols see Fig. 1.

diagrams contain states that are unstable or metastable with respect to diffusion, and these are marked as such. It is easier to understand the relationships between different tricritical or double-endpoint lines if their unstable parts are shown, too. This is also true of the critical lines themselves where features, such as the crossing and exchange of branches,[17] that occur in unstable parts of the phase diagram have important consequences on the stable phase behavior.

EQUATION OF STATE AND MIXING RULES

The Redlich–Kwong equation of state is used with its original temperature dependence:

$$P = \frac{RT}{V_m - b} - \frac{aT^{-0.5}}{V_m(V_m + b)}. \tag{11}$$

Its two parameters, a and b, are considered as quadratic and linear, respectively, functions of composition:

$$a = x_1^2 a_{11} + 2x_1 x_2 a_{12} + x_2^2 a_{22} \tag{12}$$

$$b = x_1 b_{11} + x_2 b_{22}. \tag{13}$$

Although the use of a quadratic mixing rule instead of Eq. (13) for the covolume is known to improve the quality of phase equilibrium predictions,[12] we restrict ourselves to the linear mixing rule, at least within the present work; the introduction of an additional parameter (b_{12}) would make the proper presentation of the results too complicated.

It is important to notice that the attraction parameter of the Redlich–Kwong equation is related to the Boyle temperature T^* by

$$a = RT^{*1.5} b, \tag{14}$$

whereas the attraction parameter of the van der Waals equation is proportional to T^*:

$$a_{\mathrm{vdW}} = RT^* b. \tag{15}$$

Hence Eq. (12) is not a van der Waals mixing rule. For simple equations of state like Eq. (11), the Boyle temperature is a fixed multiple of the critical temperature.

Equations (12) and (13) contain five substance-dependent parameters. As we are interested in the topology of phase diagrams only, and not in absolute pressure and temperature values, the mixtures are characterized by three dimensionless parameter ratios:

$$\xi = \frac{b_{22} - b_{11}}{b_{22} + b_{11}}, \tag{16}$$

$$\zeta = \frac{d_{22} - d_{11}}{d_{22} + d_{11}}, \tag{17}$$

$$\lambda = \frac{d_{22} - 2d_{12} + d_{11}}{d_{22} + d_{11}}. \tag{18}$$

The d_{ik} are cohesive energy densities defined by

$$d_{ik} = \frac{T_{ik}^* b_{ik}}{b_{ii} b_{kk}}. \tag{19}$$

If the van der Waals relation (15) is inserted into Eqs. (17)–(19), the parameter definitions of van Konynenburg and Scott are recovered. Thus it is ensured that ξ, ζ, and λ have the same physical meaning in this work and in that of van Konynenburg and Scott.[5]

Throughout the following, the subscript "1" refers to the component with the smaller covolume.

RESULTS

Molecules of equal size

For mixtures with $\xi = 0$ many thermodynamic relations become much simpler than usual. In that case it is possible to evaluate the conditions of azeotropy analytically; the result for the azeotropic mole fraction is

$$x_1^{az} = \frac{a_{11} - a_{22}}{a_{22} - 2a_{12} + a_{11}}. \tag{20}$$

Hence, if azeotropy occurs, the azeotropic mole fraction is independent of temperature. Since the mole fraction is subject to the condition $0 < x_1^{az} < 1$, the condition for azeotropy in terms of dimensionless parameters is $\lambda > +\zeta$ for positive azeotropy and $\lambda < -\zeta$ for negative azeotropy.

For mixtures of equal-sized molecules the covolume is a constant. This makes it possible to evaluate the conditions for a zero-temperature endpoint analytically. The result is

$$\lambda = 1 - (1 - \zeta)\left(\frac{1}{2}\left(1 + \left(\frac{1+\zeta}{1-\zeta}\right)^{3/2}\right)\right)^{2/3}. \tag{21}$$

For λ values below the value given by Eq. (21) only classes I and V can occur.

Figure 5 shows a λ vs ζ map for mixtures of equal-sized molecules. As the numbering of the components is arbitrary in this case, the diagram is symmetric with respect to the ordinate. This diagram is very similar to the one obtained by van Konynenburg and Scott for the van der Waals equation. The only striking difference is the existence of class IV behavior below the abscissa; this is not observed for the van der Waals equation.

There are three tricritical lines in Fig. 5: one at positive ζ, one at negative ζ, and one coinciding with the ordinate. The vicinity of the intersection point of these three lines has been called the shield region by Griffiths and co-workers[3,4]; here the special classes II-A*, III-A*, and III-A** can be found (but not III*). This intersection point, however, does not mark a critical state of higher order; the three tricritical mole fractions are different, and furthermore the tricritical state on the vertical line is at a different pressure, too.

The two outer tricritical lines become metastable above λ values of approximately 0.34 . The limits of stability are tricritical endpoints. They also mark the ends of the boundary lines of the shield region (lines of coexistence of a critical phase and two noncritical ones). These lines have been omitted in Fig. 5; for a more detailed description of the shield region see Refs. 3–5 and 8.

In the diagrams presented here tricritical lines and double-endpoint lines terminate for two reasons: for physical reasons (e.g., because the pressure becomes zero) or for technical reasons (e.g., because rounding errors increase for $x_1 \to 1$ or $x_1 \to 0$, causing the search algorithm to fail). Endpoints due to physical reasons are marked in the diagrams.

The tricritical lines and the double-endpoint lines do not unite, but intersect, thus forming a very narrow domain of class IV* behavior between them. At the intersection point the mole fractions x_1^c and x_1^a, which are associated with the double-endpoint line, both converge to the tricritical mole

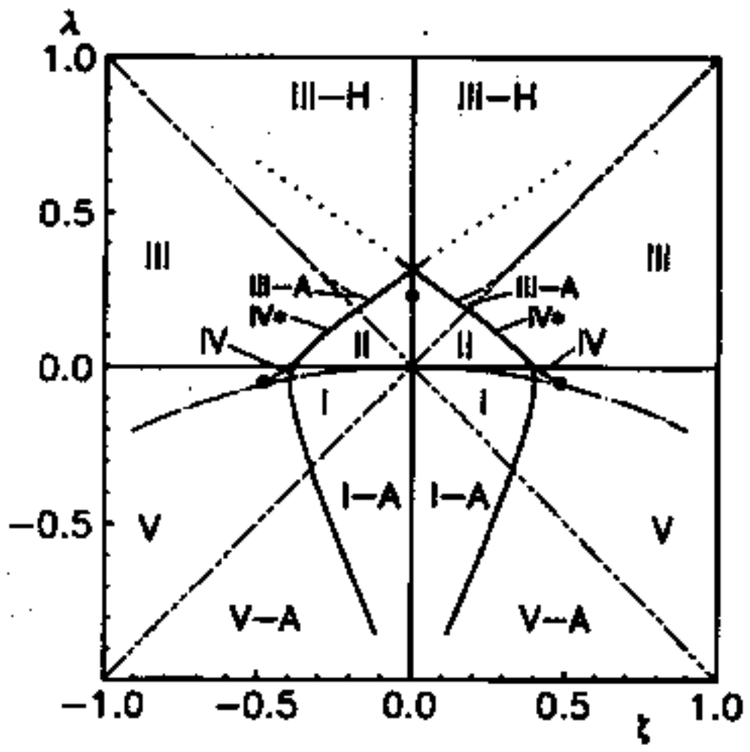

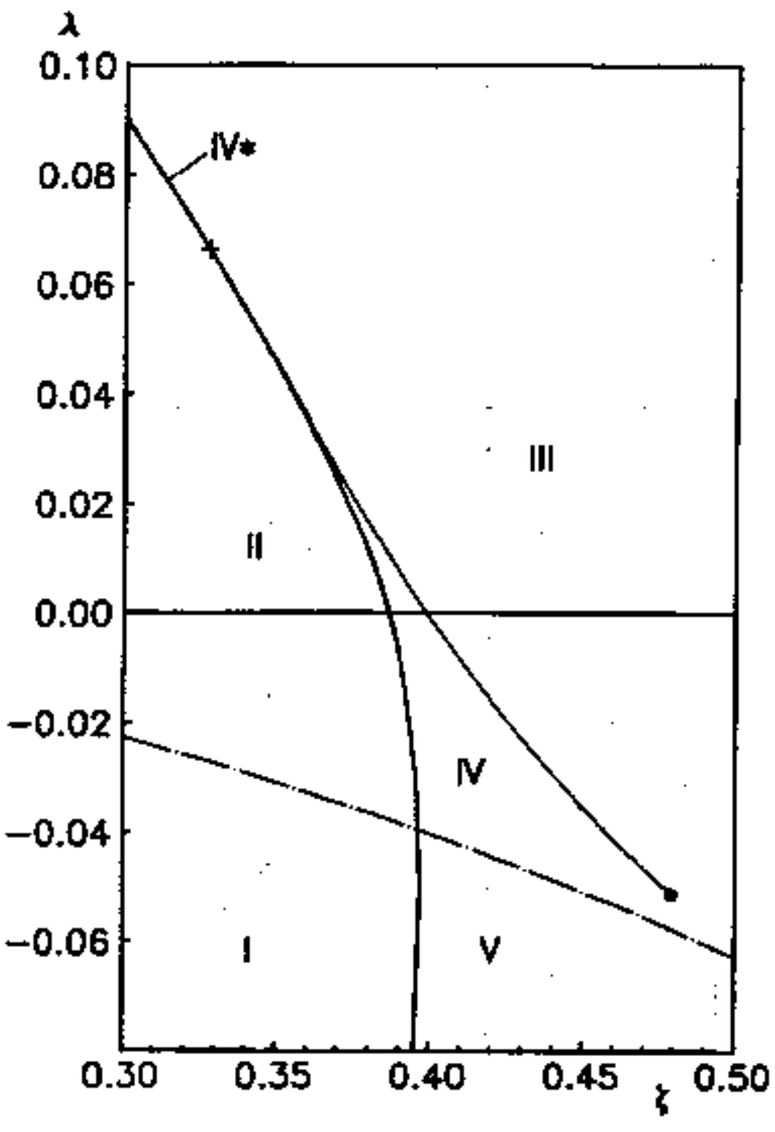

FIG. 5. λ vs ζ map for mixtures of equal-sized molecules ($\xi = 0.0$) bold: tricritical lines, thin: double-endpoint lines; solid: stable, dotted: metastable, dashed: unstable; -·-: line of zero-temperature endpoints; O: line termination; -··-: limits of azeotropy.

fraction (Fig. 6). Usually, tricritical points are generated from class IV or IV* phase diagrams by letting the length of a three-phase line shrink to zero; two critical lines meet at these tricritical points. At the intersection point, however, three critical lines and a three-phase line meet (Fig. 7) at a tricritical point. This is strongly reminiscent of symmetrical tricritical behavior, though there is no obvious symmetrical relationship between the interaction parameters. Indeed, the two boundaries that *intersect* at a point in Redlich–Kwong and van der Waals mixtures *coincide* in the three-component lattice gas,[3,4] with the consequent disappearance of classes IV and IV*, and form a line of such symmetrical tricritical points which is then the boundary between classes II and III.

A real fluid exhibiting phase behavior characteristic of this intersection point would be experimentally interesting

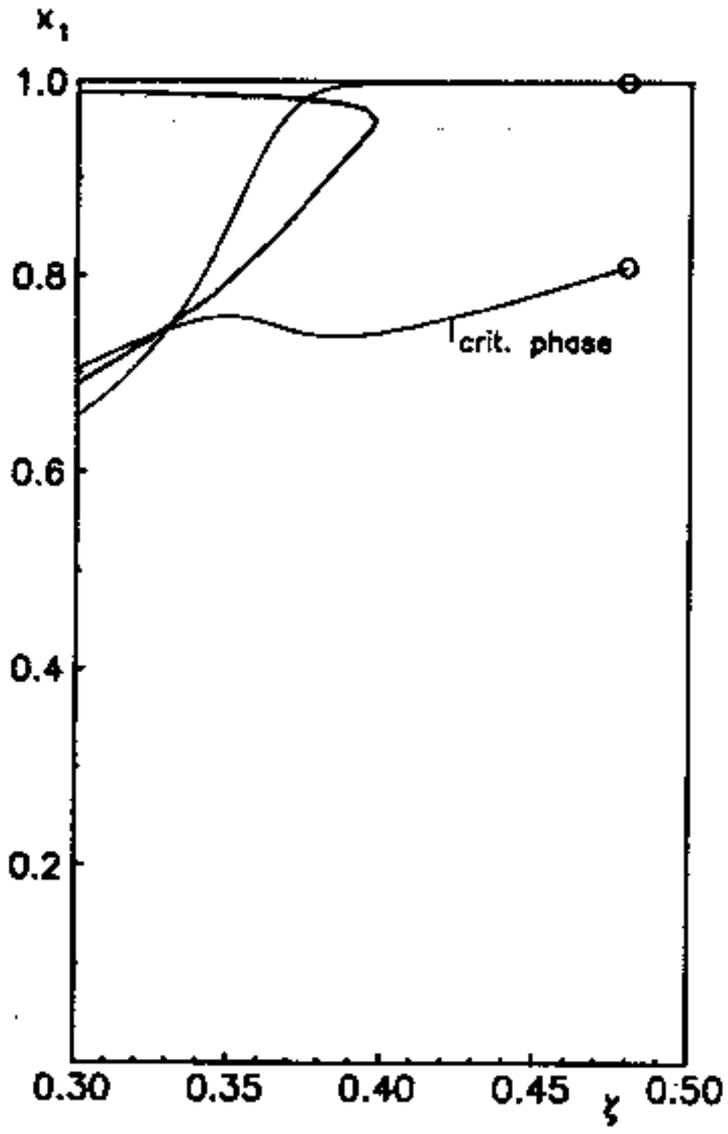

FIG. 6. Mole fractions associated with tricritical and double-endpoint lines for mixtures with equal-sized molecules. For an explanation of symbols see Fig. 5.

since one could study the approach to a tricritical point by simply changing the temperature of an appropriately prepared system.

For the van der Waals equation this point lies on the geometric mean line,[4,5] and Meijer,[18] who suggests the name van Laar point, has used this simplification to study the critical behavior in this region analytically.

Finally, we note that the critical lines form a cusp at the location of a critical azeotrope. This is in accordance with the findings for van der Waals mixtures. As discussed in recent literature,[8,9] the limits of azeotropy mentioned above are not the limits of heteroazeotropy for class III. In analogy to results obtained for the Lennard-Jones fluid, there exists a narrow domain of azeotropic behavior (III-A) between the heteroazeotropic domain III-H and the plain class III. The boundary line between III-A and III-H is a line of critical azeotropic endpoints; for Redlich–Kwong fluids it does not run into the shield region.

Molecules with similar sizes

In order to demonstrate the phase behavior of mixtures containing molecules of slightly differing sizes, we have per-

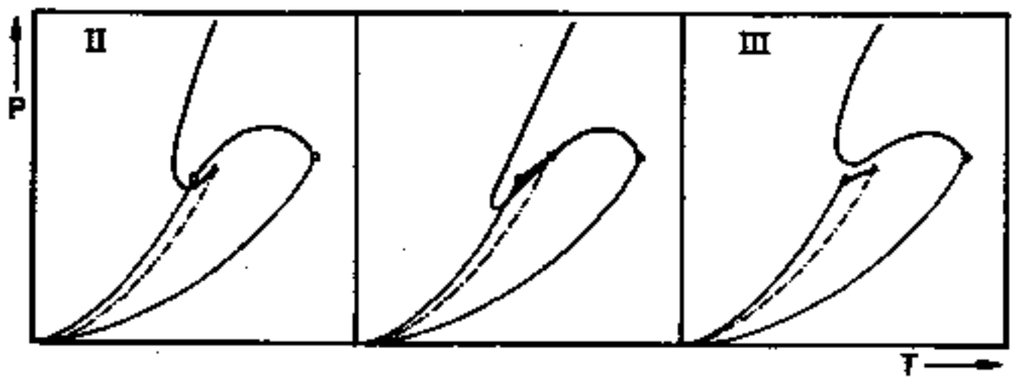

FIG. 7. Symmetric tricritical point as transition state between class II and III. For an explanation of symbols see Fig. 1.

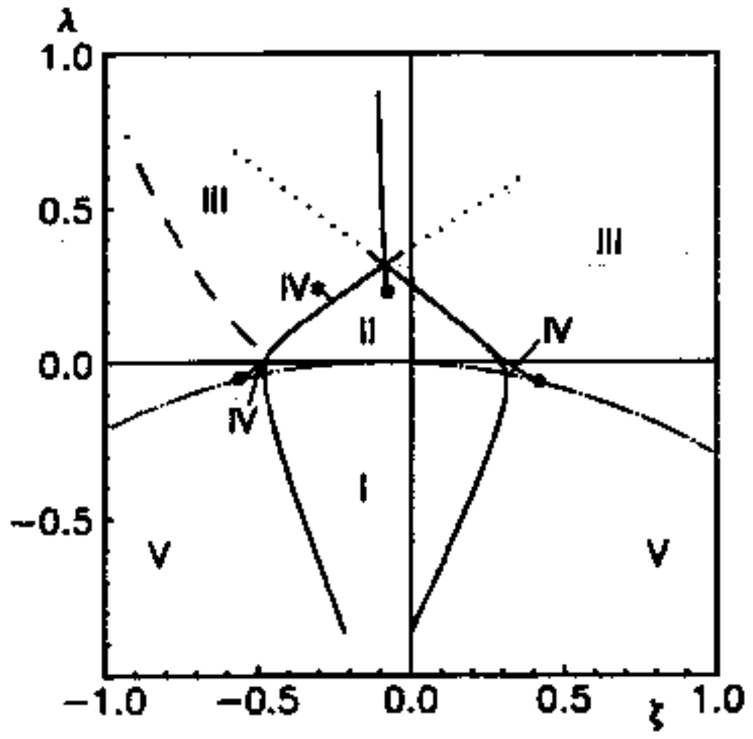

FIG. 8. λ vs ζ map for mixtures with covolume ratio $\xi = 0.1$. For an explanation of symbols see Fig. 5.

formed calculations at $\xi = 0.1$ and $\xi = 0.2$ (Figs. 8 and 9). In contrast to mixtures of equal-sized molecules, the tricritical and double-endpoint lines are no longer symmetrical about the ordinate, but are displaced to lower ζ values. The domains of the different phase diagram classes are arranged in the same way as before. In the vicinity of the "intersection point" of the three tricritical lines there is again a "shield region" where the classes II-A*, III-A**, etc., can be observed. Again, the outer tricritical lines become metastable above the shield region.

The intersection point of tricritical line and double-endpoint line at negative ζ is again a true van Laar point, which has a topology as in Fig. 7. At positive ζ, the situation is different: The intersection point—if it exists at all—is shifted into or beyond the shield region. The mole fractions of the double-endpoint line do not converge to the tricritical mole fraction (Fig. 10). Furthermore, the tricritical pressure seems to be slightly higher than the double-endpoint pressure. All this indicates that there is no symmetric tricritical point at positive ζ. However, the pressure difference is so small (0.016 %) that it is at the limit of our present numeri-

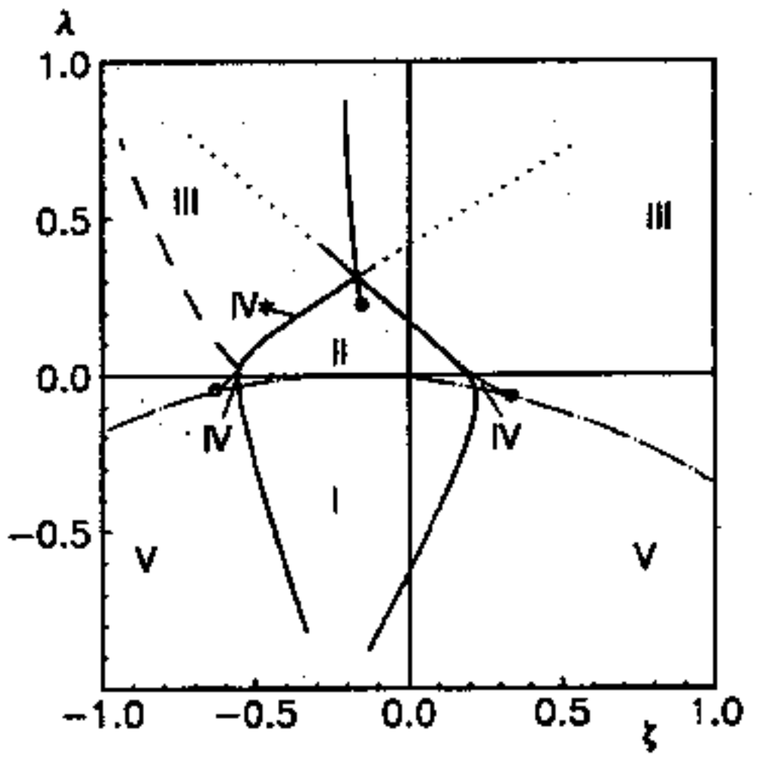

FIG. 9. λ vs ζ map for mixtures with covolume ratio $\xi = 0.2$. For an explanation of symbols see Fig. 5.

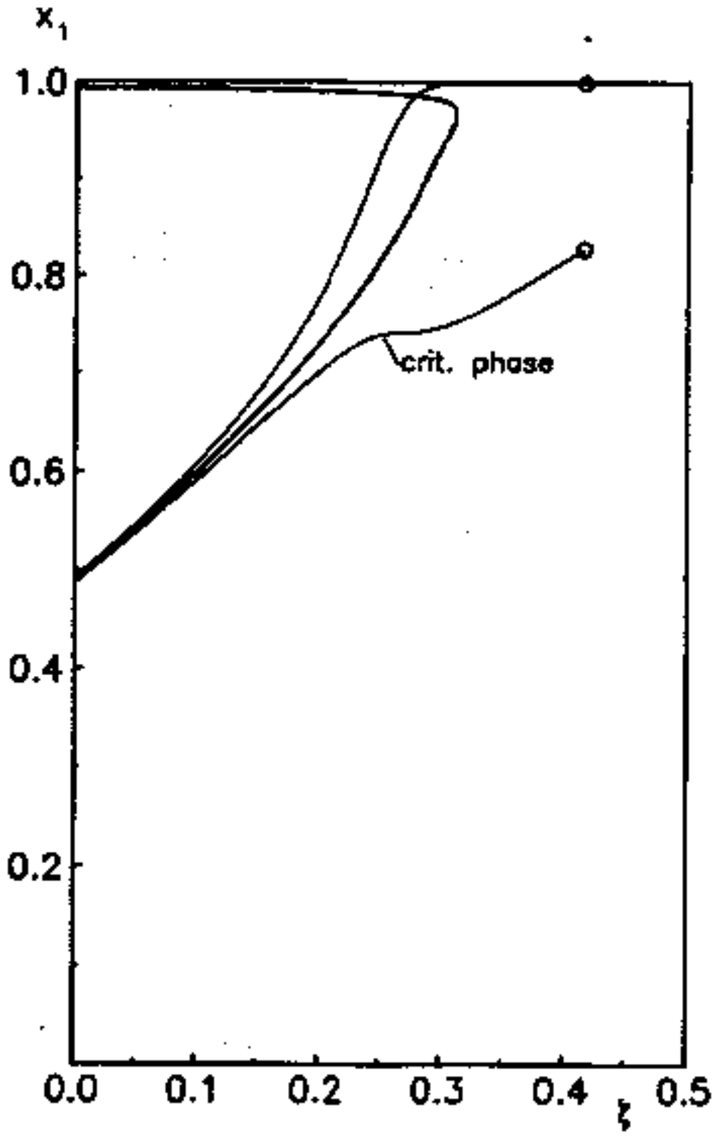

FIG. 10. Mole fractions associated with tricritical and double-endpoint lines for mixtures with $\xi = 0.1$. For an explanation of symbols see Fig. 5.

cal resolution. For all studied mixtures with $\xi > 0$, an extremely narrow domain of class IV behavior extends up to the shield region. The critical endpoints of the phase diagrams in the upper portion of this domain are so close to each other that they are distinguishable from symmetric tricritical states (Fig. 7) only by extreme numerical efforts.

An interesting feature of these mixtures is the existence of an unstable tricritical line at negative ζ. With increasing size difference, this tricritical line grows towards higher ζ values, but then turns back. In λ vs ζ diagrams (Fig. 9) a cusp is formed, whereas x_1 vs ζ diagrams show a smooth curve. Beyond the cusp, the tricritical line is metastable; it is associated with very large molar volumes and with pressures below the three-phase line.

Molecules with different sizes

From Figs. 11 and 12 it is clear that the λ vs ζ map looks rather similar for positive ζ. However, the left corner of the kite-shaped figure is changed very much. The tricritical line forming this corner splits into two branches. This is also evident from the x_1 vs ζ diagram (Fig. 13). The lower branch goes from large negative λ values towards zero, then becomes metastable and finally, through a cusp, unstable. The upper branch runs from the shield region either towards an endpoint (Fig. 11) or to very negative ζ values (Fig. 12). Near this corner there are relatively broad domains of class IV and class IV* behavior adjacent to each other. This seems to be a contradiction, because IV and IV* differ in the connectivity of critical lines and should therefore be separated by a tricritical line. However, a close investigation of the phase diagrams in these domains shows that the two domains are separated by a narrow strip in which a special kind

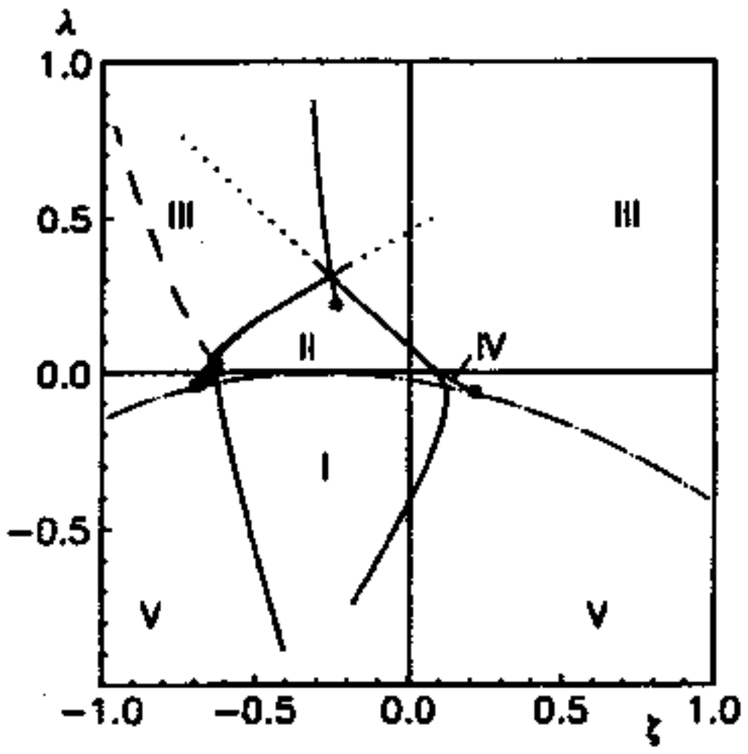

FIG. 11. λ vs ξ map for mixtures with covolume ratio $\xi = 0.3$. For an explanation of symbols see Fig. 5.

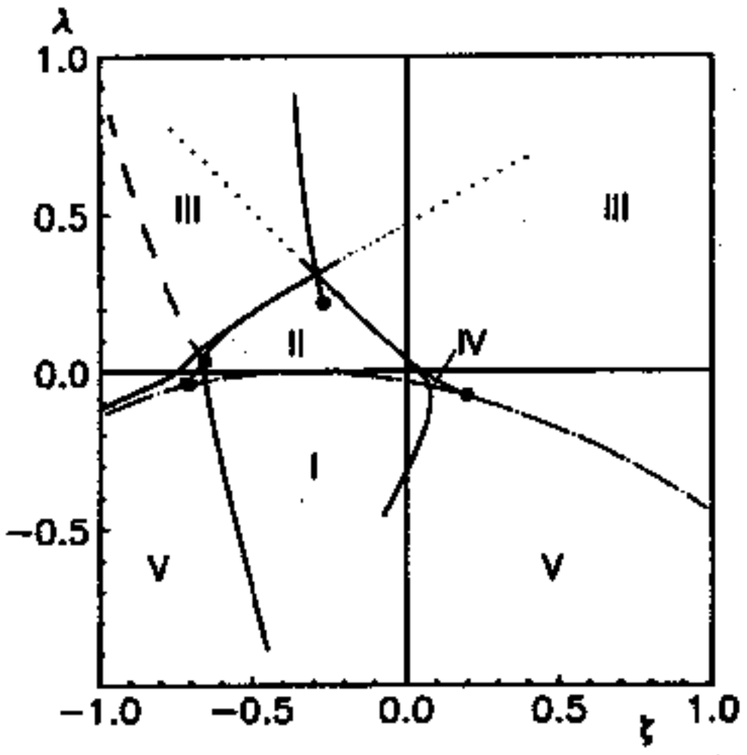

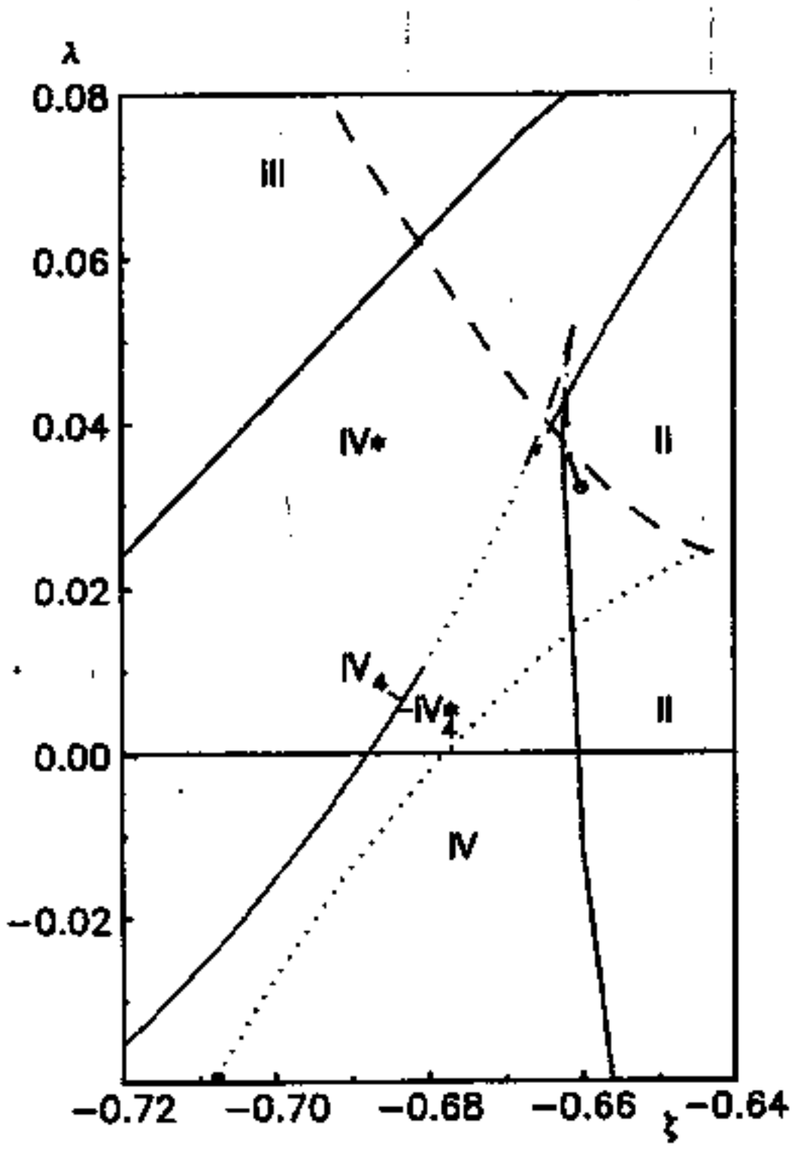

FIG. 12. λ vs ξ map for mixtures with covolume ratio $\xi = 0.3457$. For an explanation of symbols see Fig. 5.

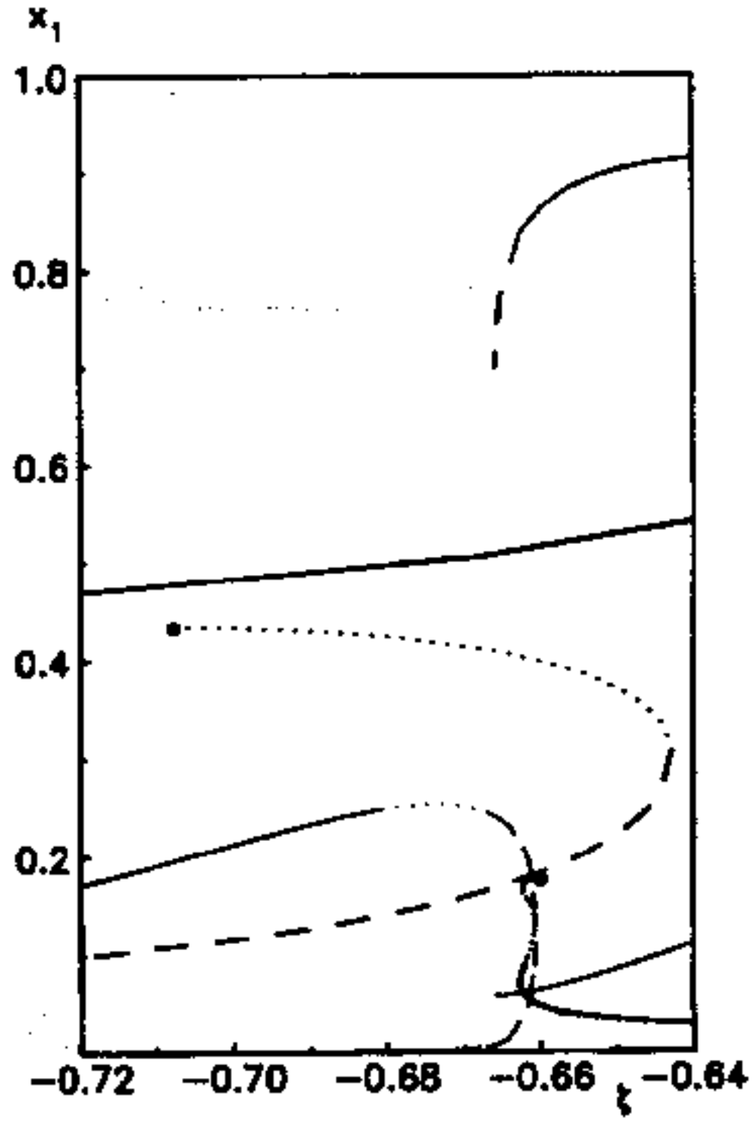

FIG. 13. Mole fractions associated with the tricritical and double-endpoint lines in Fig. 12(b). For an explanation of symbols see Fig. 5.

of phase behavior can be observed which has not been reported in the work of van Konynenburg and Scott (Fig. 14). The most important feature of this class, which we will refer to as IV_4, is a four-phase state. Depending on the curvature of the critical line originating at C_h, there are two subclasses: In the simple case, this critical line runs into a lower critical endpoint; in the case IV_4^*, it touches or penetrates another three-phase line, thereby generating an additional pair of critical endpoints. (Strictly speaking, there are different three-phase lines which might be penetrated; hence several subclasses should be possible, which differ in the way in which the critical lines and the three-phase lines are connected. However, a pursuit of all the ramifications on the phase diagram classification system would be beyond the scope of this work.)

Such a phase behavior could not be found for mixtures with smaller covolume ratios. In this context, it is interesting to note that the "three-component lattice model" of Furman *et al.*[3] contains a domain of four-phase coexistence (termed "type II" by the authors) in a part of their global phase diagram map which corresponds to the area covered in Fig.

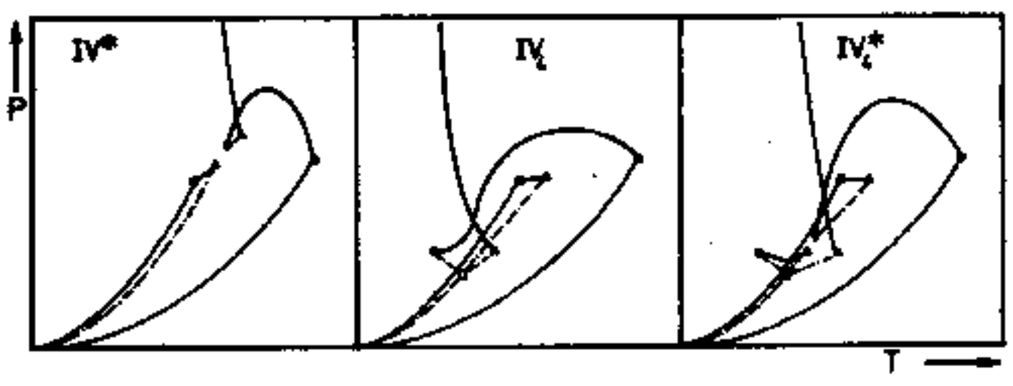

FIG. 14. Schematic representation of phase diagrams belonging to subclasses of class IV.

12(b), though, of course, no size difference occurs in their model.

The high-volume tricritical line mentioned before is also present in these systems. P–T phase diagrams with parameter sets located close to, but above this tricritical line are of a distorted class IV behavior, where the critical line from C_k and that from C_m seem to cross each other before joining at still lower pressures. But all these interesting states are physically unstable or at best metastable.

DISCUSSION

In the case of molecules of equal size, the global phase diagrams obtained with the Redlich–Kwong equation are very similar to those obtained for the van der Waals fluid or for the Lennard-Jones fluid. Not only is the arrangement of the various domains the same, but also the parameter values of certain features, e.g., the shield region, seem to be very similar. In contrast to recent results for the Lennard-Jones fluid, we have not found any trace of class VI or class VII behavior in the vicinity of the van Laar pointa. Furthermore, we have shown that several lines appearing in the global phase diagrams may have physical endpoints and do not always extend all over the diagram. For the Redlich–Kwong fluid with quadratic mixing rules for the attraction parameters and linear mixing rules for the covolumes, zero-temperature endpoints constitute a nontrivial boundary between several classes. For molecules of different sizes, the topology of the global phase diagram changes considerably; new subclasses of phase diagrams containing a four-phase state were found.

It is surprising that such a simple equation of state as the Redlich–Kwong equation leads to such a variety of phase diagram classes, especially when the investigation is not restricted to equal-sized molecules. It must be asked, of course, how "real" the computed phase diagrams are. In practice the parameters of an equation of state should reflect molecular properties and cannot be set to any desired value. It is possible, however, to simulate a continuously variable binary mixture by adjusting composition ratios in appropriate ternary or quaternary (quasibinary) mixtures.[19–24] Therefore experimentally realizing tricritical states, four-phase states, etc. is not *a priori* unrealistic.

A more important result is, perhaps, that some of the more unusual phase diagram classes (IV^*, IV_4), which are of negligible importance for mixtures of equal-sized molecules, may become quite important for molecules of different sizes. The relatively large ζ values required to bring about the special phase behavior are no obstacle: For simple equations of state, the "cohesive energy density" defined by Eq. (19) is proportional to the critical pressure; the parameter ζ may therefore be regarded as a ratio of critical pressures. The combination of large positive ξ and large negative ζ, which is required for IV_4 behavior, can be achieved by mixtures of water with some heavier hydrocarbons or alkanols; such systems may even be of technical importance. It may be worth to note that a few real mixtures which according to their Redlich–Kwong parameters should belong to class IV_4 exhibit class VI behavior.

It is interesting to note that while the symmetric three-component model of Furman *et al.*[3] contains four-phase states of "type II," the van der Waals model of these authors,[4] which is derived from the three-component model by changing the mixing entropy function, does not exhibit such behavior. The binary Redlich–Kwong model of this work, which is conceptually very close to the van der Waals model, again contains type II four-phase states, but only for large size differences and very negative values of ζ. For positive ζ values or for very high λ values no such states could be detected. It would be interesting to determine whether the van der Waals equation shows similar behavior with large size differences or whether this is actually a consequence of the equation of state itself. A full comparison of the two equations of state awaits a more complete study of size-difference effects in van der Waals mixtures.

At present, it is not quite clear to what extent the observed phase behavior depends on the temperature function of the equation of state and on the mixing rules (or rather mixing theory). This will be the object of future investigations.

ACKNOWLEDGMENTS

The authors wish to thank Professor P. H. E. Meijer (Catholic University of America, Washington, D.C., USA) and Dr. J. M. H. Levelt Sengers [National Institute of Science and Technology (formerly NBS), Gaithersburg, MD, USA] as well as Professor J. de Swaan Arons (Technical University Delft, NL) for fruitful discussions and many helpful suggestions. Financial support by the Deutsche Forschungsgemeinschaft and by the Fonds der Chemischen Industrie e.V. is gratefully acknowledged. One of us (U.K.D.) has received a stipend from the Karl–Winnacker–Stiftung.

APPENDIX

Conditions for a critical point

The standard thermodynamic formulation of the critical conditions for a binary mixture, i.e., $G_{2x} = G_{3x} = 0$, is of little practical use for the computation of critical states because these derivatives are defined at constant pressure and temperature whereas the natural variables of the equation of state are molar volume and temperature. It is possible, however, to transform the above conditions into equations of a more useful form by means of Jacobian determinants:

$$G_{2x} = A_{2x} - \frac{A_{Vx}^2}{A_{2V}}. \tag{A1}$$

Here A_{ijVkx} is an abbreviation for

$$\left(\frac{\partial^{i+j+k} A_m}{\partial T^i \partial V_m^j \partial x_1^k}\right).$$

If A_{2V} is positive (this is not the case for critical azeotropes!), Eq. (A1) leads to the critical condition

$$A_{2V}A_{2x} - A_{Vx}^2 = 0. \tag{A2}$$

If this equation is fulfilled and A_{2V} is positive, the second critical condition can be transformed into

$$A_{3x}A_{2V}^2 - 3A_{V2x}A_{Vx}A_{2V} + 3A_{2Vx}A_{Vx}^2 - A_{3V}A_{2x}A_{Vx} = 0. \quad \text{(A3)}$$

The Redlich–Kwong equation makes the evaluation of the critical conditions very easy: All derivatives of the Helmholtz energy required in Eqs. (A2) and (A3) have the functional form

$$A_{ijx} = p_{ij}T + q_{ij}T^{-0.5}, \quad \text{(A4)}$$

where p_{ij} and q_{ij} depend on V_m and x_1 only. If these two variables are specified, Eq. (A2)—after insertion of Eq. (A4)—turns out to be a quadratic equation for $T_c^{1.5}$. With the critical temperature known, it is possible to evaluate Eq. (A3). The coefficients p_{ij} and q_{ij} are:

$$p_{2V} = +\frac{R}{(V_m-b)^2} \quad q_{2V} = -\frac{a(2V_m+b)}{V_m^2(V_m+b)^2}, \quad \text{(A5)}$$

$$p_{Vx} = -\frac{2Rb'}{(V_m-b)^2} \quad q_{Vx} = +\frac{a'(V_m+b)-ab'}{V_m(V_m+b)^2}, \quad \text{(A6)}$$

$$p_{2x} = +\frac{Rb''}{V_m-b} + \frac{Rb'^2}{(V_m-b)^2} + \frac{R}{x_1x_2}, \quad \text{(A7a)}$$

$$q_{2x} = -\ln\frac{V_m+b}{V_m}\frac{a''b^2-abb''-2a'bb'+2ab'^2}{b^3} - \frac{2a'b'+ab''}{b(V_m+b)} + \frac{ab'^2(2V_m+3b)}{b^2(V_m+b)^2}. \quad \text{(A7b)}$$

a and b are obtained from the mixing rules (12) and (13). Their derivatives are:

$$a'' = \frac{d^2a}{dx_1^2} = 2(a_{11}-2a_{12}+a_{22}) \quad \text{(A8)}$$

$$a' = \frac{da}{dx_1} = x_1a'' + 2(a_{12}-a_{22}). \quad \text{(A9)}$$

The derivatives of b have analoguous definitions (here: $b_{12} = \frac{1}{2}(b_{11}+b_{22})$, hence $b''=0$).

A recommendable numerical procedure is to keep x_1 fixed and to vary V_m between b and $4b$ in small steps, each time calculating T_c and evaluating (A3). A change of sign indicates that a critical point is near; it can then be determined more precisely by means of a regula falsi iteration.

Calculation of tricritical points

Whereas the calculation of G_{2x} from Eq. (A1) and Eqs. (A4)–(A9) requires only a moderate mathematical effort, the formula for G_{3x} is already of a tremendous complexity, and the analytical calculation of the higher derivatives up to G_{6x} is almost hopeless. We have therefore computed the higher derivatives by numerical differentiation. It is important, however, to apply numerical differentiation to the residual part of G_m only, because all derivatives of the ideal mixing term diverge for $x_1 \to 1$ or $x_1 \to 0$, causing a severe loss of numerical precision. The equations used for the computation of the Gibbs energy derivatives are

abbreviations:

$$g_{2x}(x_1) = G_{2x}/RT - x_1\ln x_1 - x_2\ln x_2 \quad \text{(A10)}$$

$g_n = g_{2x}(x_1+nh)$ h: differentation increment,

$$\frac{G_{3x}}{RT} = \frac{1}{360h}[256(g_{+1}-g_{-1}) - 40(g_{+2}-g_{-4}) + (g_{+4}-g_{-4})] - x_1^{-2} + x_2^{-2} \quad \text{(A11)}$$

$$\frac{G_{4x}}{RT} = \frac{1}{720h^2}[1024(g_{+1}-2g_0+g_{-1}) - 80(g_{+2}-2g_0+g_{-2}) + (g_{+4}-2g_0+g_{-4})] + 2x_1^{-3} + 2x_2^{-3}, \quad \text{(A12)}$$

$$\frac{G_{5x}}{RT} = \frac{-1}{48h^3}[64(g_{+1}-g_{-1}) - 34(g_{+2}-g_{-2}) + (g_{+4}-g_{-4})] - 6x_1^{-4} + 6x_2^{-4} \quad \text{(A13)}$$

$$\frac{G_{6x}}{RT} = \frac{-1}{48h^4}[256(g_{+1}-2g_0+g_{-1}) - 68(g_{+2}-g_0+g_{-2}) + (g_{+4}-2g_0+g_{-4})] + 24x_1^{-5} + 24x_2^{-5}. \quad \text{(A14)}$$

These derivatives were used with a Marquardt-type algorithm to locate tricritical states.

Calculation of double critical endpoints

An expression for the slope of a three-phase line at a critical endpoint is unlikely to be found in thermodynamic textbooks, therefore, a short derivation is given.

For a binary fluid mixture, the total differential of the molar Gibbs energy is given by

$$dG_m = -S_m\,dT + V_m\,dP + G_x\,dx_1. \quad \text{(A15)}$$

The chemical potentials can be calculated from

$$\mu_i = G_m - (-1)^i(1-x_i)G_x \quad \text{with } i = 1,2. \quad \text{(A16)}$$

This leads to the following expressions for the differentials of the chemical potentials:

$$d\mu_1 = -(S_m + x_2S_x)dT + (V_m + x_2V_x)dP + x_2G_{2x}\,dx_1$$
$$d\mu_2 = -(S_m - x_1S_x)dT + (V_m - x_1V_x)dP - x_1G_{2x}\,dx_1. \quad \text{(A17)}$$

At a critical endpoint two phases, a critical and an auxiliary phase, are in equilibrium. We postulate now

$$d\mu_i^c = d\mu_i^a \quad \text{with } i = 1,2. \quad \text{(A18)}$$

Inserting Eq. (A17) into Eq. (A18) yields a set of two linear equations. For the critical phase, G_{2x}^c vanishes, so that no term containing dx_1^c is left. The terms containing dx_1^a can be eliminated from Eq. (A18). The remaining terms can be rearranged into

$$\frac{dP}{dT} = \frac{S_m^c - S_m^a - (x_1^c - x_1^a)S_x^c}{V_m^c - V_m^a - (x_1^c - x_1^a)V_x^c}. \quad \text{(A19)}$$

This is the slope of the three-phase line at a critical endpoint in a PT–projection. For a double endpoint, this slope is the same as the slope of the critical line. Equation (4) is the mathematical representation of this condition.

Again the problem arises to calculate the derivatives V_{kx} and S_{kx}, which are defined at constant pressure, from a pressure-explicit equation of state. In analogy to Eq. (A1),

these derivatives can also be expressed through derivatives of the Helmholtz energy

$$V_x = -\frac{A_{Vx}}{A_{2V}}, \tag{A20}$$

$$V_{2x} = -\frac{1}{A_{2v}} A_{V2x} + 2A_{2Vx} V_x + A_{3V} V_x^2, \tag{A21}$$

$$S_x = -(A_{Tx} + A_{TV} V_x), \tag{A22}$$

$$S_{2x} = -(A_{T2x} + 2A_{TVx} V_x + A_{T2V} V_x^2 + A_{TV} V_{2x}). \tag{A23}$$

Calculation of zero-temperature endpoints

As the endpoint temperature decreases, so does the pressure, because the three-phase line cannot deviate too much from the vapor pressure lines. With $T \to 0$ and $P \to 0$, the molar volume of the liquid phase approaches the covolume b.

Under these circumstances, only the attractive term within G_m

$$\frac{a}{b\sqrt{T}} \ln\left(1 + \frac{b}{V_m}\right)$$

contributes to its curvature. With $V_m \to b$, it is only necessary to check the curvature of a/b with respect to x_1

$$\frac{d^2(a/b)}{dx_1^2} = b^{-3}(a''b^2 - abb'' - 2a'bb' + 2ab'^2) = 0. \tag{A24}$$

If the mixing rule for the covolume parameter b is linear, as it is assumed in this work [Eq. (13)], the term containing b'' vanishes, and the expression for the third order derivative is

$$\frac{d^3(a/b)}{dx_1^3} = 3b^{-4}(-a''b^2b' + 2a'bb'^2 - 2ab'^3) = -\frac{3b'}{b}\frac{d^2(a/b)}{dx_1^2}. \tag{A25}$$

If the second order derivative is zero, the third order derivative vanishes, too. It is therefore sufficient to evaluate the second order derivative. For molecules of equal sizes this can be done analytically [see Eq. (21)], but usually the numerical solution of Eq. (A24) presents no problem.

[1] P. H. van Konynenburg, Ph.D. thesis, University of California, Los Angeles, 1968.
[2] R. L. Scott and P. H. van Konynenburg, Discuss. Faraday Soc. 49, 87 (1970).
[3] D. Furman, S. Dattagupta, and R. B. Griffiths, Phys. Rev. B 15, 441 (1977).
[4] D. Furman and R. B. Griffiths, Phys. Rev. A 17, 1139 (1978).
[5] P. H. van Konynenburg and R. L. Scott, Philos. Trans. R. Soc. London Ser. A 298, 495 (1980).
[6] P. Clancy, K. E. Gubbins, and C. G. Gray, Discuss. Faraday Soc. 66, 116 (1978).
[7] G. Jackson, J. S. Rowlinson, and C. A. Lang, J. Chem. Soc. Faraday Trans. I 82, 3461 (1986).
[8] V. A. Mazur, L. Z. Boshkov, and V. B. Fedorov, Dokl. Akad. Nauk SSSR 282(1), 137 (1985).
[9] L. Z. Boshkov and V. A. Mazur, Russ. J. Phys. Chem. 60, 16 (1986).
[10] L. Z. Boshkov, Dokl. Akad. Nauk SSSR 294(4), 901 (1987).
[11] O. Redlich and J. N. S. Kwong, Chem. Rev. 44, 233 (1949).
[12] U. Deiters and G. M. Schneider, Ber. Bunsenges. Phys. Chem. 80, 1316 (1976).
[13] J. S. Rowlinson and F. L. Swinton, *Liquids and Liquid Mixtures*, 3rd ed. (Butterworths, London, 1982), pp. 193, 211, 311.
[14] A. Barker and W. Fock, Discuss. Faraday Soc. 15, 188 (1953).
[15] J. C. Wheeler and G. R. Andersen, J. Chem. Phys. 73, 5778 (1981).
[16] P. Clancy and K. E. Gubbins, Mol. Phys. 44, 581 (1981).
[17] P. H. E. Meijer, M. Keskin, and I. L. Pegg, J. Chem. Phys. 88, 1976 (1988).
[18] P. H. E. Meijer, J. Chem. Phys. 90, 448 (1989).
[19] J. Specovius, M. A. Leiva, R. L. Scott, and C. M. Knobler, J. Phys. Chem. 85, 2313 (1981).
[20] M. C. Goh, J. Specovius, R. L. Scott, and C. M. Knobler, J. Chem. Phys. 86, 4120 (1987).
[21] E. Fernandez-Fassnacht, A. G. Williamson, A. Sivaraman, R. L. Scott, C. M. Knobler, J. Chem. Phys. 86, 4133 (1987).
[22] I. L. Pegg, M. C. Goh, R. L. Scott, and C. M. Knobler, Phys. Rev. Lett. 55, 2320 (1985).
[23] I. L. Pegg, Kinam A 6, 3 (1984).
[24] C. M. Knobler and R. L. Scott, in *Phase Transitions and Critical Phenomena*, edited by C. Domb and R. L. Scott (Academic, London, 1984), Vol. 9, p. 1.